Pergamon

PII: S0967-0645(96)00023-9

Deep-Sea Research II, Vol. 43, No. 4–6, pp. 907–931, 1996

0967–0645/96 $15.00 + 0.00

Dynamics of picophytoplankton, ultraphytoplankton and bacteria in the central equatorial Pacific

BRIAN J. BINDER,*‡ SALLIE W. CHISHOLM,* ROBERT J. OLSON,† SHEILA L. FRANKEL* and ALEXANDRA Z. WORDEN*‡

(*Received* 12 *February* 1995; *in revised form* 3 *December* 1995; *accepted* 1 *February* 1996)

Abstract—Pico- and ultraplankton are known to contribute significantly to overall biomass and primary productivity in the "high nutrient–low chlorophyll" waters of the equatorial Pacific. In order to understand the dynamics of this community on ecologically relevant time-scales, we examined the abundance, distribution and cellular characteristics of *Prochlorococcus*, *Synechococcus*, eukaryotic ultraphytoplankton and heterotrophic bacteria during two 20-day time-series at 0°N, 140°W in the spring and fall of 1992 (JGOFS time-series cruises, TS-I and TS-II). *Prochlorococcus* was numerically dominant among the autotrophic groups considered, with mean cell concentrations in surface waters on the order of 1.4×10^5 cells ml^{-1}. *Synechococcus* and ultraphytoplankton abundances were 17–30-fold lower than those of *Prochlorococcus*, and heterotrophic bacterial abundances were 5–7-fold higher (during TS-I and TS-II, respectively). Daily cell abundances for all groups varied by factors of 1.5–2 within each time-series. Depth-integrated *Prochlorococcus* abundance averaged over each time-series was 25% lower during TS-II relative to TS-I; ultraphytoplankton abundance was 42% higher during the same period. *Prochlorococcus* and ultraphytoplankton both contributed significantly to the estimated total autotrophic biomass; *Synechococcus* contributed relatively little. Estimated total photosynthetic pico- plus ultraplankton biomass was on average 30% higher than heterotrophic bacterial biomass.

Changes in the fluorescence and light scatter properties of individual *Prochlorococcus* cells were observed during the passage of a tropical instability wave during TS-II, and are hypothesized to reflect a physiological response among these cells to that event. Examination of bulk properties alone (e.g. cell numbers or total red fluorescence) would not have revealed these physiological changes.

Lower bounds for *Prochlorococcus*-specific growth rates were calculated based on the DNA distributions of these populations at dusk. These rates were maximal at 15 or 30 m depth, where they approached one doubling per day. Changes in *Prochlorococcus* forward angle light scatter (FALS) from dawn to dusk were well correlated with these estimates of specific growth rate, an observation that allowed us to relate measurements of FALS to cell volume for *Prochlorococcus*. Copyright © 1996 Elsevier Science Ltd

INTRODUCTION

The flux of CO_2 from the equatorial Pacific Ocean accounts for an important part of the total flux of carbon out of the world's oceans and into the atmosphere (Feely *et al.*, 1987). In the simplest terms, this flux results from the upwelling and warming of high-CO_2 water in this region. Acting against this physically driven outward flux of CO_2 is the so-called "biological pump" (Longhurst, 1991). The strength of this pump depends not only on the

*Ralph M. Parsons Laboratory, Massachusetts Institute of Technology, Cambridge, MA 02139, U.S.A.
†Department of Biology, Woods Hole Oceanographic Institution, Woods Hole, MA 02543, U.S.A.
‡Present address: Department of Marine Sciences, University of Georgia, Athens, GA 30602–2206, U.S.A.

rate of primary production, but also on the structure of the biological community, insofar as this structure influences the extent to which fixed carbon is recycled (resulting in no net pumping) or is exported out of the system (resulting in a loss of carbon from the local system).

The importance of small cells to overall primary production in oligotrophic marine environments is well established (see reviews in Stockner and Antia, 1986; Chisholm, 1992; Weisse, 1993). The limited data available for the central and eastern equatorial Pacific indicate that despite the persistence of high concentrations of N and P in surface waters, pico- and ultraplankton contribute significantly to primary production in this area as well. Chavez (1989) showed that generally more than 50% of the chlorophyll standing stock was contributed by the $<1\ \mu m$ size class, and more than 80% by the $<5\ \mu m$ class (which accounted for approximately 80% of the total primary productivity). Similarly, Peña *et al.* (1990) showed that the <1 and $<10\ \mu m$ size classes contributed, respectively, from 20 to 51%, and from 76 to 87% of the total chlorophyll *a* at 135°W. Most recently, Bidigare and Ondrusek (1996) estimated that between 81 and 92% of total chlorophyll *a* was contributed by the $<2\ \mu m$ size class at 140°W. The dominance of relatively small photosynthetic cells in waters replete with N and P has been taken as indirect evidence that primary production in this region is limited by iron or some other trace nutrient (Chisholm, 1992).

These data support the notion that small cells contribute significantly to primary production in the equatorial Pacific, but they provide little insight into the dynamics of these populations over time. Given the extremely dynamic nature of the physical system in this area (on time scales ranging from days to years), it is not unreasonable to expect that variability in the biological community and, therefore in the efficiency of the biological pump, may also be significant. The two JGOFS equatorial Pacific "time-series" cruises undertaken in March–April and October 1992 at 140°W were designed in part to assess this variability (Murray *et al.*, 1993).

Although the original purpose for carrying out a time-series in both the spring and the fall was to address seasonal changes in the central equatorial Pacific, these cruises must be viewed in the context of the inter-annual climatic variations that influenced conditions in 1992 (Barber *et al.*, 1994). During the March–April time-series (referred to hereafter as TS-I) El Niño conditions (e.g. anomalously high sea-surface temperatures and 20°C isotherm depths) were evident, whereas during the October series (TS-II) anomalously strong "cold tongue" conditions prevailed (Barber *et al.*, 1994; Murray *et al.*, 1994). Despite these differences, upwelling persisted at 140°W throughout both time-series, and nitrate was always present at the surface.

Murray *et al.* (1994) summarized the shifts in biological characteristics that occurred within and between the two time-series at 140°W. Low-frequency changes, between TS-I and TS-II, included an increase in water column-integrated primary production, specific primary production and (to a lesser extent) chlorophyll *a* (Barber *et al.*, 1994). Systematic high-frequency changes within each time-series were not evident during TS-I but were clear during TS-II, and were associated with the passage of a tropical instability wave (TIW) (Murray *et al.*, 1994). These changes included an increase in primary production and chlorophyll *a*, but no apparent change in the specific (per chlorophyll) rate of primary production. The factors ultimately responsible for these high- and low-frequency changes remain to be established. However, there is an indication that the proximal cause may involve shifts in the structure of the primary producer community.

In this paper, we consider the abundance and dynamics of picoplankton and

ultraplankton groups over the course of the two 20-day time-series, and examine the extent to which these may reflect or contribute to the observed ecosystem-level changes.

MATERIALS AND METHODS

Samples were taken during the March–April and October 1992 JGOFS Equatorial Pacific Time-series at 0°N, 140°W (R.V. *Thompson* cruises 8 and 12). TS-I extended from 23 March to 9 April 1992 (Julian days 83–100) and TS-II from 2 to 21 October 1992 (Julian days 276–295). Thirty-liter Niskin bottles from daily dawn or dusk CTD casts were sampled into dark 250-ml polypropylene bottles. Unless otherwise noted, the data presented in this paper are from the dawn casts. Within approximately 20 min of drawing these samples, aliquots were preserved in 0.12% glutaraldehyde (final concentration) and frozen in liquid nitrogen for later analysis on-shore (Vaulot *et al.*, 1989; Olson *et al.*, 1993).

In preparation for flow cytometric analysis, samples were stained using a modification of the protocol of Monger and Landry (1993). Immediately following sample thawing (at room temperature), 0.5-ml aliquots were stained with the DNA-specific fluorochrome Hoechst-33342 (0.5 $\mu g\,ml^{-1}$ final concentration). Stained samples were held at room temperature in the dark for 1 h prior to analysis; no significant changes in cell number, red autofluorescence or Hoechst fluorescence were detectable between 15 min and 4 h of staining under these conditions (data not shown). Just prior to analysis, known volumes of two standard bead stocks were added: 0.57-μm diameter blue-excitable beads ("Fluoresbrite YG", Polysciences, Inc.) and 0.46-μm diameter UV-excitable beads ("Fluoresbrite BB"). These beads were used to determine cell abundances, and as internal fluorescence and light scatter standards (Olson *et al.*, 1993).

Samples were analyzed using dual beam flow cytometry with a modified EPICS-753 (Coulter Corp.) equipped with a 38-mm focal length quartz plano-convex focusing lens (Olson *et al.*, 1990a), a "Biosense" flow cell and a forward angle light scatter PMT detector (Hamamatsu R1923) with an extra-wide obscuration bar (estimated angle of collection, 7–15°). Two Ar-ion lasers (Coherent, Inc.) were employed: one tuned to 488 nm (800 mW output) and the other to 360–365 nm (300 mW output).

Blue forward angle light scatter (FALS) and 90° light scatter were measured through 488-nm band-pass filters (10-nm band width). Fluorescence signals all passed a 488-nm dichroic and a 418 long-pass filter; red fluorescence (from chlorophyll) was the 488 nm-excited signal passing a 680-nm band-pass filter (40 nm bandwidth, Omega Optical "680 DF40"), orange fluorescence (from phycobiliproteins) was the 488 nm-excited signal passing a 580-nm band-pass filter (50 nm bandwidth, "580 DF50") and blue fluorescence (from Hoechst/DNA) was the UV-excited signal passing a 470 nm short-pass filter (with strong blocking at 488; "470 EFSP"). Log-integrated signals were collected for all parameters.

Prochlorococcus, *Synechococcus* and ultraphytoplankton were recognized according to their light scatter and fluorescence characteristics as described previously (Olson *et al.*, 1990a, 1993) [Fig. 1(A)–(D)]. In this paper, we define "ultraphytoplankton" operationally as that population of cells with high red fluorescence and light scatter, but no detectable orange fluorescence (arising from phycoerythrin) [Fig. 1(A) and (B)]. The majority of cells in this group ranged in diameter between approximately 1 and 2 μm (based on microscopic examination of sorted cells). However, our analysis also included in this group those (larger) cells that were off-scale in red fluorescence and light scatter. Most such cells had diameters of the order of 3 μm, and as a group they generally accounted for $<20\%$ of the total

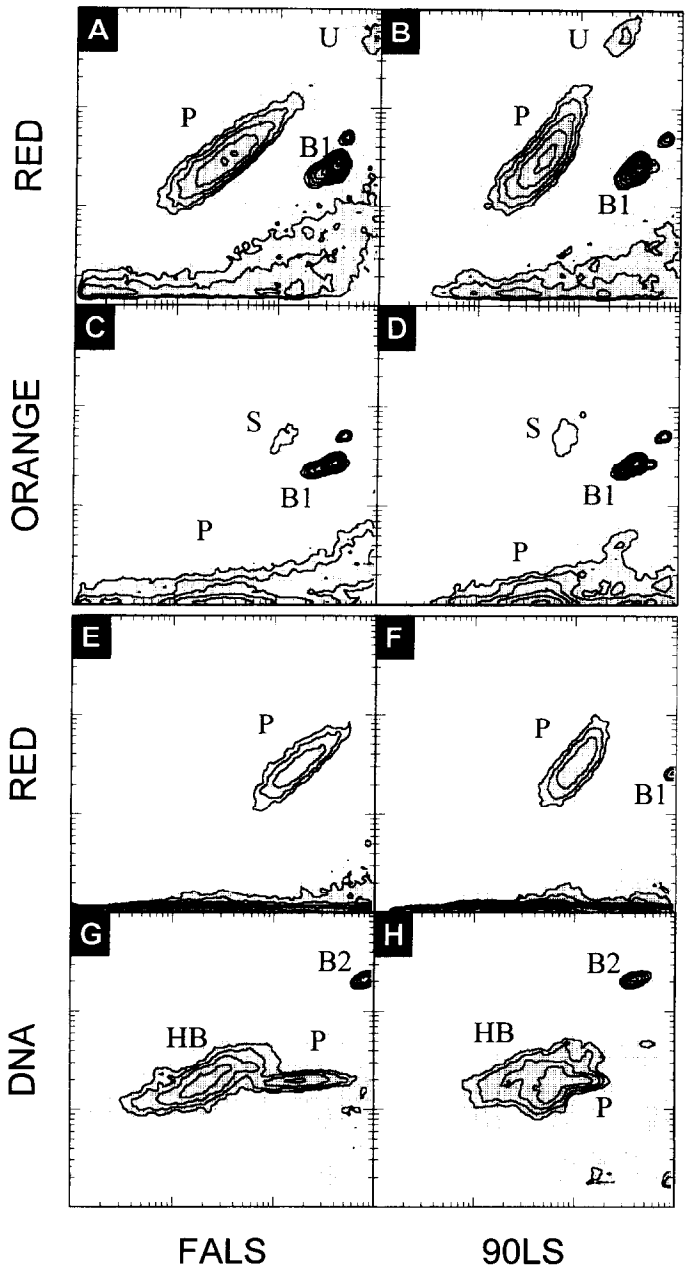
A
U
P
B1
B
U
P
B1
RED
C
S
B1
P
D
S
B1
P
ORANGE
E
P
F
P
B1
RED
G
B2
HB
P
H
B2
HB
P
DNA
FALS
90LS

ultraphytoplankton cell count (DuRand and Olson, 1996). We assume that this group corresponds roughly to the eukaryotic photosynthetic "ultraplankton" (Shapiro and Guillard, 1986).

In addition to these photosynthetic groups, heterotrophic bacteria could be discriminated on the basis of their blue fluorescence, light scatter properties and lack of detectable red or orange fluorescence [Fig. 1(E)–(H)]. Note that we were able to resolve the FALS of bacterial cells in these samples [Fig. 1(G)]. This parameter is more directly related to cell size than is 90° light scatter, and it provides for better discrimination between different populations [compare Fig. 1(G) and (H); see also the Results and Discussion]. Detection and enumeration of heterotrophic bacteria in marine samples using flow cytometry have been demonstrated previously by Robertson and Button (1989), Monfort and Baleux (1992) and Monger and Landry (1993).

The large difference between the FALS of bacteria and of *Synechococcus* and ultraphytoplankton precluded measuring both at the same time. Therefore, each stained sample was run sequentially at two light scatter sensitivities (adjusted by changing the high voltage settings of the FALS and 90° light scatter PMTs). The "standard" sensitivity level (corresponding to that described in Olson *et al.*, 1993) was sufficient to keep *Prochlorococcus* cells above the FALS baseline, but low enough to keep *Synechococcus* cells on the scale [Fig. 1(A) and (C)]. Even at this reduced sensitivity, ultraphytoplankton cells were often off-scale in FALS, although they were largely on-scale in 90° light scatter [Fig. 1(A) and (B)]. For this reason, ultraphytoplankton FALS data are not presented. Approximately 120 μl of the sample were run at this setting, and the resulting data used for *Prochlorococcus*, *Synechococcus* and ultraphytoplankton analysis. Higher light scatter sensitivity settings were used to analyze heterotrophic bacteria [Fig. 1(G) and (H)]. At these settings, most of the *Synechococcus* and ultraphytoplankton were off-scale in FALS. Approximately 40 μl of the sample (corresponding to 0.8×10^4–3.2×10^4 bacterial cells) were run in this configuration.

Flow cytometry data were collected in list mode and analyzed with software ("CytoPC") provided by D. Vaulot (Station Biologique, Roscoff, France). FALS and 90° light scatter and red and orange fluorescence were normalized to the 0.57 μm standard beads, and blue fluorescence to the 0.46 μm beads. For the analysis of *Prochlorococcus* DNA distributions, DNA data originally collected in log mode were re-binned on a linear scale, and

Fig. 1. Typical flow cytometric signatures obtained in this study. The sample was from 15 m depth, at dawn on Julian day 284. Axes represent relative magnitude of each parameter on an approximately 3-decade log scale. Contours show relative frequency of cells with a given combination of characteristics. Contour levels in all panels correspond to 2, 4, 8, 16, etc., counts; dots correspond to >1 count. (A)–(D) "Standard sensitivity": (A) red (chlorophyll-derived) fluorescence vs FALS (related to size); (B) red fluorescence vs 90° light scatter; (C) orange (phycobiliprotein-derived) fluorescence vs FALS; and (D) orange fluorescence vs 90° scatter. (E)–(H) "High sensitivity": (E) red fluorescence vs FALS; (F) red fluorescence vs 90° light scatter; (G) blue fluorescence (corresponding to Hoechst-stained DNA) vs FALS; and (H) blue fluorescence vs 90° light scatter. P, *Prochlorococcus*; S, *Synechococcus*; U, ultraphytoplankton; HB, heterotrophic bacteria; B1 and B2, 0.57 and 0.46 μm standard beads (note that because of large differences in refractive index, bead diameters cannot be used to estimate cell size). *Synechococcus* cells are present in (A) and (B), but are not distinguishable from the much more numerous *Prochlorococcus* cells in these views of the data. They are easily identified in (C) and (D) based on their orange fluorescence. Heterotrophic bacteria are identified at the high-sensitivity settings as those cells with blue fluorescence but without red fluorescence [(G) and (H)]; these cells fall on the red baseline in (E) and (F). Note that bacterial cells are resolved in both FALS and 90° light scatter. *Prochlorococcus* cells (identified on the basis of their red fluorescence combined with their relatively low light scatter) appear in panel (G) as a tight horizontal streak.

deconvoluted into so-called "g1", "s" and "g2" subpopulations (corresponding to G1, S and G2 + M phases of the eukaryotic cell cycle; Binder and Chisholm, 1995) using ModFit software (Verity Software House, Inc.). Minimum daily specific growth rates were calculated from dusk samples using the equation $\mu_{min} = \ln[1 + P(s + g2)]$, where P(s + g2) is the proportion of "s" and "g2" cells at dusk (Antia *et al.*, 1990; Vaulot, 1992).

Depth integrations were calculated assuming a linear change in the parameter of interest between adjacent sampling depths; integrations were calculated from the surface to 120 m (approximately the 0.1% light level).

Data from this paper are available on the U.S. JGOFS database via the World Wide Web (http:\\wwwl.whoi.edu/jgofs.html).

RESULTS AND DISCUSSION

Cell abundance—vertical distribution

The vertical abundance distributions of each photosynthetic group and of heterotrophic bacteria changed little over the course of each time-series, but differences between the two series were evident, particularly among *Prochlorococcus* and ultraphytoplankton (Fig. 2). In general, the abundances and distributions observed for all groups were consistent with those reported for the same location approximately 1 month prior to each time-series (Landry *et al.*, 1996).

Among the photosynthetic populations, *Prochlorococcus* was by far the numerically dominant group at all depths. *Prochlorococcus* numbers in the upper 30 m were approximately equal during both time series, averaging approximately 1.4×10^5 ml^{-1} [Fig. 2(A) and Table 1]. Below this depth, differences between the two cruises became evident with cell abundances at 120 m more than 20-fold higher during TS-I than during TS-II. This difference was reflected in the depth-integrated *Prochlorococcus* numbers which, on average, were 25% lower during TS-II than during TS-I (Table 1). The lack of a significant subsurface *Prochlorococcus* abundance maximum during either of these time-series is

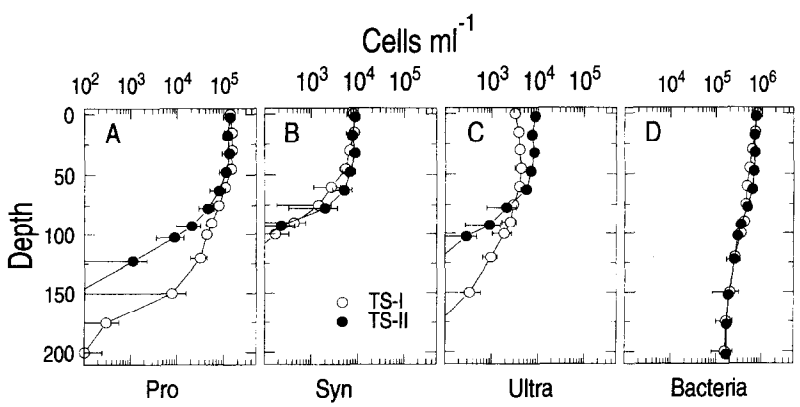

Fig. 2. Depth profiles of mean cell abundance at dawn during TS-I (○) and TS-II (●) for (A) *Prochlorococcus*, (B) *Synechococcus*, (C) ultraphytoplankton and (D) heterotrophic bacteria. Each point represents the mean among all the dawn casts analyzed; error bars represent the SD among those casts ($n = 7$ for TS-I and $n = 9$ for TS-II). Note the change in scale in (D).

Table 1. Comparison of surface and water column-integrated daily mean cell abundances and variation during TS-I and TS-II (mean ± SD). Surface values are 0–30 m means; water column values are integrated to 120 m (approximately 0.1% surface light intensity)

	n	*Prochlorococcus*	*Synechococcus*	Ultraphytoplankton	Bacteria
Surface abundance					
		($\times 10^5$ cells ml^{-1})	($\times 10^3$ cells ml^{-1})	($\times 10^3$ cells ml^{-1})	($\times 10^5$ cells ml^{-1})
TS-I	7	1.47 ± 0.34	7.65 ± 1.72	3.64 ± 0.62	7.05 ± 1.16
TS-II	9	1.34 ± 0.37	8.56 ± 1.95	8.34 ± 1.60	7.13 ± 1.11
Change (TS-I→TS-II)*		(−9%)	(+12%)	+129%	(+1%)
Means†		NS	NS	$p < 0.002$	NS
Variances‡		NS	NS	$p < 0.05$	NS
Water column abundance					
		($\times 10^9$ cells cm^{-2})	($\times 10^7$ cells cm^{-2})	($\times 10^7$ cells cm^{-2})	($\times 10^9$ cells cm^{-2})
TS-I	7	1.20 ± 0.16	4.15 ± 0.30	3.77 ± 0.50	6.06 ± 0.74
TS-II	9	0.90 ± 0.23	5.29 ± 1.45	5.39 ± 0.97	6.42 ± 0.80
Change (TS-I→TS-II)*		−25%	(+27%)	+42%	(+6%)
Means†		$p < 0.01$	NS	$p < 0.01$	NS
Variances‡		NS	$p < 0.002$	NS	NS

*Change in time-series average, values in parentheses not significant.
†Mann–Whitney U-test comparing time-series means.
‡Two-tailed *F*-test comparing time-series variances.

consistent with other data for this area (Chavez *et al.*, 1991; Landry *et al.*, 1996) and with observations of different high surface-nitrate waters (Olson *et al.*, 1990a; Vaulot *et al.*, 1990; Shimada *et al.*, 1993).

The vertical distribution of ultraphytoplankton also showed significant differences between the two time-series: surface concentrations during TS-II were more than 2-fold higher than during TS-I, while the concentrations at depth were considerably lower [Table 1 and Fig. 2(C)]. On a depth-integrated basis, ultraphytoplankton abundance was 42% higher during TS-II (Table 1).

In contrast to *Prochlorococcus* and ultraphytoplankton, depth profiles of *Synechococcus* did not differ between the two time-series [Fig. 2(B)]. Mean abundance was approximately 8×10^3 ml^{-1} in the top 30 m, but decreased rapidly below that depth; *Synechococcus* concentrations were < 100 cells ml^{-1} below 100 m. There was no significant difference in surface- or depth-integrated *Synechococcus* abundance between the two time-series.

Abundance profiles for heterotrophic bacteria were relatively consistent within and between time-series [Fig. 2(D) and Table 1], with cell concentrations dropping by a factor of 5 from the surface to 200 m (from approximately 7×10^5 to 1.5×10^5 ml^{-1}). Ducklow *et al.* (1995) reported similar trends in the vertical distribution of bacterial abundance (measured as acridine orange direct counts) at midday during the same cruises. However, in contrast to the results of that study (in which mean surface bacteria abundance was 25% higher during TS-II than during TS-I), we found no significant difference in mean bacterial abundance between the two cruises (Table 1). This discrepancy reflects the fact that while our flow cytometric measurements of bacterial abundance were not significantly different from the values determined by Ducklow *et al.* (1995) during TS-I (Wilcoxin's signed rank test), they were systematically lower than those of Ducklow *et al.* during TS-II (average

difference = 27%; $p < 0.001$). The reasons for this discrepancy are unknown at present. It is possible that the differences in bacterial abundance between the two cruises at midday noted by Ducklow *et al.* (1995) were not present at dawn (when we sampled). Alternatively, these results may point to differences in the two methods of estimating bacterial abundance. Previous comparisons between bacteria cell counts using epifluorescence microscopy and flow cytometry have shown good agreement between the two approaches (Monfort and Baleux, 1992; Monger and Landry, 1993), but there is evidence that the use of different DNA stains (as is the case here) could result in different estimates of bacterial abundance (Suzuki *et al.*, 1993).

On average, *Prochlorococcus* cell concentrations in the upper 30 m were approximately 20% of heterotrophic bacteria concentrations. In contrast, surface *Prochlorococcus* numbers in the oligotrophic North Pacific have been reported to be as high as 45% of the heterotrophic bacterial numbers (Campbell *et al.*, 1994).

Cell abundance—temporal variation

Despite the relative consistency of the shape of vertical abundance profiles within each time-series, changes in absolute abundance did occur over the course of each. Thus, while mean *Prochlorococcus* abundance at the surface was approximately the same for both cruises, daily abundance numbers ranged over at least a factor of 2 within each cruise [Fig. 3(A) and Table 1]. Variations in *Synechococcus* and ultraphytoplankton surface concentrations were of the same order; heterotrophic bacterial concentrations ranged over a factor of about 1.5 [Fig. 3(B)–(D)].

For the most part, patterns in areal cell inventories, integrated to 120 m (approximately the 0.1% light depth), reflected the patterns observed in surface cell abundances [Fig. 3(E)–(H)]. However, there was a marked reduction in the variance of the daily *Synechococcus* depth-integrated cell numbers during TS-I relative to TS-II [Fig. 3(F) and Table 1]. Changes in *Synechococcus* abundance at the surface during TS-I were largely balanced by relatively subtle changes in the depth distribution of these cells.

The depth-integrated *Prochlorococcus* abundances observed in this study were higher than those generally found in the Sargasso Sea and northwest Atlantic Ocean (Olson *et al.*, 1990a), but only about half the reported value for the subtropical North Pacific (Campbell and Vaulot, 1993). In contrast, the observed *Synechococcus* abundances were generally lower than wintertime Sargasso Sea numbers, comparable to summertime numbers and greater than subtropical North Pacific numbers (Olson *et al.*, 1990a; Campbell and Vaulot, 1993).

Previously published data suggest that, in open-ocean environments, *Synechococcus* abundance is highest when nitrate is present at or near the surface. In the northern Sargasso Sea, for example, *Synechococcus* abundance is highest in February when winter mixing supplies nitrate to the surface, and lowest in the summer when the water column is well stratified (Olson *et al.*, 1990a). In the subtropical North Pacific, where nitrate is rarely detectable in the euphotic zone at any time, *Synechococcus* abundances are uniformly low (Campbell and Vaulot, 1993). Therefore, the *Synechococcus* abundances reported here for the equatorial Pacific, where nitrate was always relatively high at the surface, are somewhat lower than expected. In much the same way, the ratio of *Prochlorococcus*:*Synechococcus* abundance observed (~ 20) is higher than might have been expected based on nutrient concentrations alone. In the Sargasso Sea this ratio ranges from ~ 1 to ~ 10 in the winter

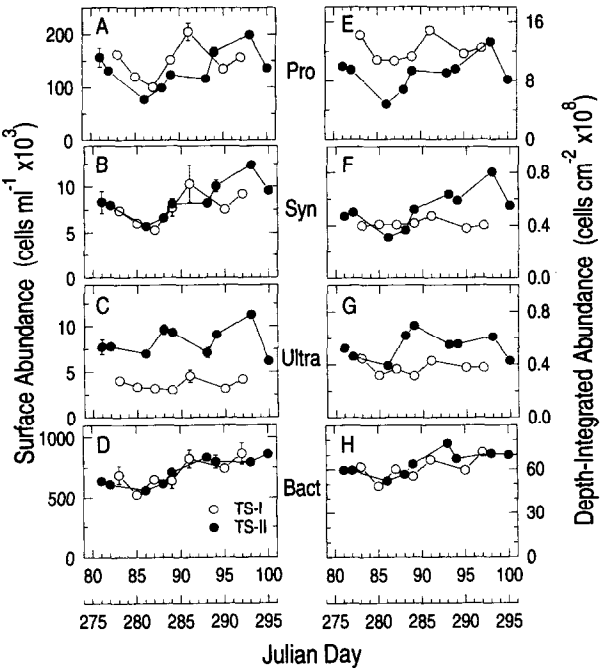

Fig. 3. Cell abundance at the surface (0–30 m) [(A)–(D)], or integrated to 120 m (~0.1% light level) [(E)–(H)], vs time during TS-I (○) and TS-II (●). (A) and (E), *Prochlorococcus*; (B) and (F), *Synechococcus*; (C) and (G), ultraphytoplankton; and (D) and (H), heterotrophic bacteria. In (A)–(D) points represent the mean cell concentration between 0 and 30 m depth at dawn, error bars correspond to the SE of that mean ($n=2$ or 3 for all points). Note that there is no relationship between the TS-I and TS-II time axes: they are placed arbitrarily for ease of comparison between the two cruises.

and the summer, respectively (Olson *et al.*, 1990a; Li *et al.*, 1992), while in the subtropical Pacific it is approximately 100 (Campbell and Vaulot, 1993). In contrast to the observations reported here, *Synechococcus* depth-integrated abundance in the western equatorial Pacific during active upwelling appears to be of the order of winter Sargasso Sea values, as might have been expected on the basis of surface N concentration [Blanchot *et al.*, 1992 (as tabulated in Campbell and Vaulot, 1993)]. Nevertheless, our observations indicate that high surface nitrate does not necessarily result in the development of large *Synechococcus* populations in open-ocean environments.

There was a remarkably good correlation between the abundance of *Prochlorococcus* and *Synechococcus* at the surface over both time-series ($r=0.84$, $p<0.01$) [Fig. 4(A)]. This correlation was also apparent for depth-integrated abundances during TS-II ($r=0.89$, $p<0.01$), but not during TS-I, when depth-integrated *Synechococcus* numbers varied little and appeared to be depressed relative to *Prochlorococcus* [Fig. 4(B)]. These correlations imply that, in the short term, *Synechococcus* and *Prochlorococcus* populations may be regulated in a similar manner by environmental factors. This is consistent with the observation of Bidigare and Ondrusek (1996) that divinyl chlorophyll *a* (a marker for *Prochlorococcus* spp.) and phycoerythrin (a marker for cyanobacteria) covaried during N–S transects of the equatorial Pacific. Vaulot *et al.* (1990) likewise reported a correlation

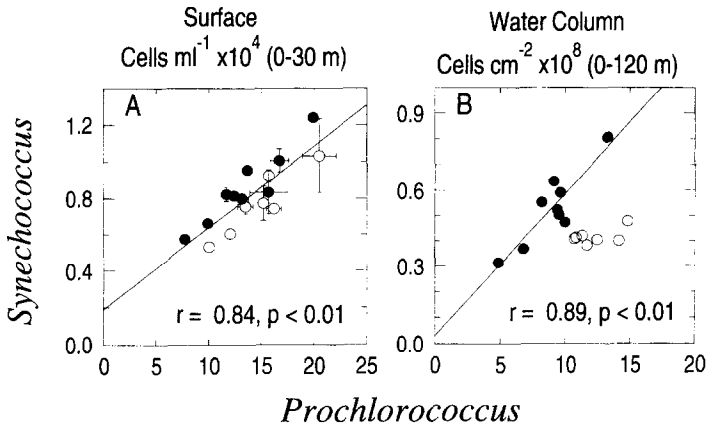

Fig. 4. The relationship between dawn surface abundance (A) or depth-integrated abundance (B) of *Prochlorococcus* and *Synechococcus* during TS-I (○) and TS-II (●). (A) Mean surface abundance ± SE, as in Fig. 3(A)–(D). Correlation statistics refer to the combined data set from TS-I and TS-II. (B) Symbols represent the single depth-integrated (0–120 m) cell numbers calculated on each day. Correlation statistics refer to the TS-II data only. The lines in both panels are from regressions that took *Prochlorococcus* and *Synechococcus* numbers as the independent and dependent variables, respectively.

between *Prochlorococcus* and *Synechococcus* abundance in the Mediterranean Sea during the winter. In contrast, it has been observed that *Synechococcus* and *Prochlorococcus* abundances tend to vary in opposite directions over larger time and space scales (Olson *et al.*, 1990a; Chisholm, 1992; Campbell and Vaulot, 1993). These two sets of observations are not mutually exclusive: it may be that the factors that regulate long-term (and broad scale) variations in the population (e.g. nutrients, light and temperature) are different to those that result in short-term (and small-scale) variation (e.g. grazing and advection).

The ultraphytoplankton cell abundances observed (particularly during TS-II), although comparable to the abundances observed by Landry *et al.* (1996) in the same area, were, on average, higher than those reported previously for most other open-ocean environments (Olson *et al.*, 1990a; Li *et al.*, 1992; Campbell and Vaulot, 1993), and overlap significantly only with wintertime values from the Mediterranean Sea and Sargasso Sea [Olson *et al.*, 1990a; Vaulot *et al.*, 1990 (as tabulated in Campbell and Vaulot, 1993)]. Therefore, these high abundances may be related to the persistence of high surface nitrate concentrations at our study site. The observation of relatively low numbers of small eukaryotes in high-nitrate western equatorial Pacific waters argues against this interpretation (Blanchot *et al.*, 1992); however, the methods used to preserve and count samples in that study may have resulted in an underestimate of ultraphytoplankton abundance (Li and Wood, 1988; Campbell and Vaulot, 1993).

Pico- and ultraphytoplankton cellular characteristics—vertical profiles

As has been observed many times before, cellular red fluorescence increased dramatically with depth in *Prochlorococcus*, *Synechococcus* and ultraphytoplankton (Fig. 5), presumably reflecting increased chlorophyll per cell at decreased light intensities (see below). The vertical profiles of fluorescence for each group were relatively invariant both within and

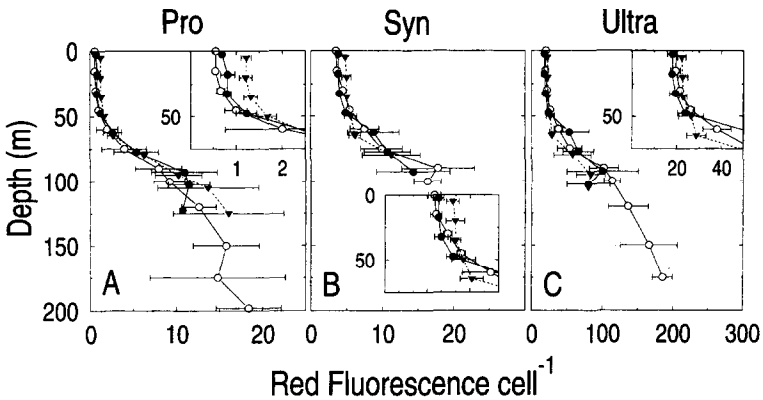

Fig. 5. Depth profiles of mean red fluorescence per cell during TS-I (○) and TS-II (●, ▼) for (A) *Prochlorococcus*, (B) *Synechococcus* and (C) ultraphytoplankton. For TS-II, profiles from days 281, 283 and 284, which were influenced by passage of the TIW, are considered separately (▼). Each point represents the mean among dawn casts, error bars represent the SD among those casts ($n = 7$ for TS-I, $n = 6$ for non-TIW TS-II and $n = 3$ for TIW TS-II). Insets show detail of same data for the upper 75 m. Data for populations of less than 100 cells ml^{-1} are considered unreliable, and are excluded from this and following figures.

between cruises. Thus, the differences noted above in vertical distributions of *Prochlorococcus* and ultraphytoplankton cell abundances between TS-I and TS-II were not reflected in the per-cell red fluorescence of these groups. Although the passage of a tropical instability wave during TS-II did appear to influence chlorophyll fluorescence profiles, particularly in the case of *Prochlorococcus*, this effect was confined to the upper 50 m of the water column (Fig. 5, broken lines) (see discussion of temporal changes below).

FALS per cell generally also increased with depth among the photosynthetic groups, particularly *Prochlorococcus* (Fig. 6), most probably reflecting an increase in average cell size with increasing depth. The much less dramatic increase in *Synechococcus* average FALS with depth is likely the result of a less pronounced change in size in this group, but may also reflect changes in the relationship between FALS and cell volume for larger cells (Morel, 1991; but see also discussion under "*Prochlorococcus* growth rates" below). As was the case for chlorophyll fluorescence, the TIW during TS-II appeared to affect *Prochlorococcus* FALS within the top 50 m or so [Fig. 6(A), broken line].

Campbell and Vaulot (1993) suggest that changes in *Prochlorococcus* red fluorescence and light scatter with depth in the subtropical Pacific may reflect shifts among *Prochlorococcus* species as well as physiological shifts within a given species (see also Moore *et al.*, 1995). In samples from intermediate depths, these authors could discern two *Prochlorococcus* populations with distinct flow cytometric signatures. We observed similar "double populations" between 60 and 100 m in many profiles during both time-series (data not shown), and hypothesize that similar shifts in *Prochlorococcus* species may have been occurring.

Pico- and ultraphytoplankton cellular characteristics—temporal changes

Mean red fluorescence and FALS of individual *Prochlorococcus*, *Synechococcus* and ultraphytoplankton cells at the surface (0–30 m) remained relatively constant over the

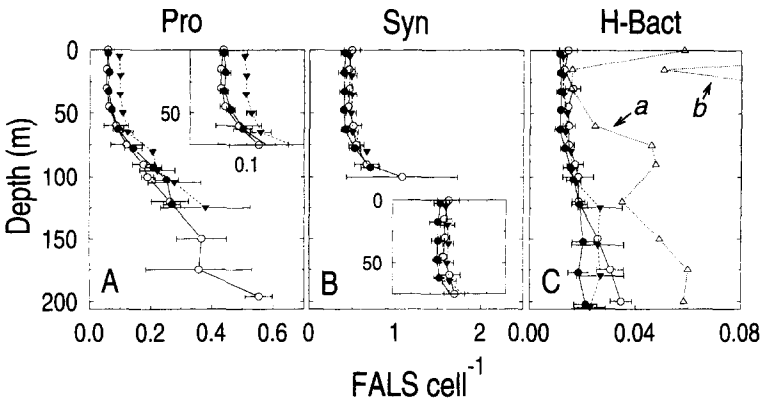

Fig. 6. Depth profiles of mean FALS per cell during TS-I and TS-II for (A) *Prochlorococcus*, (B) *Synechococcus* and (C) heterotrophic bacteria. Symbols as in Fig. 5, except in panel (C), where TS-I days 83 (*a*) and 97 (*b*) are plotted separately (see text).

course of TS-I (Fig. 7). In contrast, during TS-II, *Prochlorococcus* cells underwent dramatic changes in these parameters [Fig. 7(A) and (D)]. At the start of this time series, both red fluorescence and FALS per cell were comparable to the corresponding values during TS-I, but both increased by a factor of approximately 1.7 by day 281, returning to their initial values on day 289. These changes were largely confined to the upper 50 m of the water column [Fig. 7(A) and 8(A)], and coincided with the passage of the TIW during this time-series (Murray *et al.*, 1994). There was a hint of increases in the fluorescence of

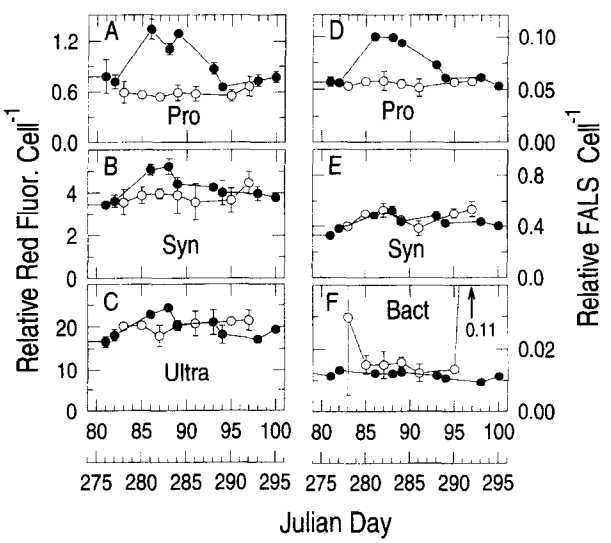

Fig. 7. Cellular red fluorescence [(A)–(C)] and FALS [(D) and (E)] in surface populations of (A) and (D) *Prochlorococcus*, (B) and (E) *Synechococcus*, (C) ultraphytoplankton and (F) heterotrophic bacteria over the course of TS-I (○) and TS-II (●). Points represent the mean value of the flow cytometrically measured per cell red fluorescence or FALS for populations at dawn between 0 and 30 m. Error bars correspond to the SE of these means ($n = 2$ or 3 for all points).

Synechococcus and ultraphytoplankton cells over the same period, although these were neither as dramatic nor as consistent as in *Prochlorococcus* [Fig. 7(B) and (C)].

Although the relationship between flow cytometrically measured red fluorescence and cellular chlorophyll content can be non-linear (Sosik *et al.*, 1989; Perry and Porter, 1989), changes in red fluorescence can yield information about the direction and magnitude of changes in chlorophyll content, particularly within a single species or group of closely related species (Veldhuis and Kraay, 1990; Moore *et al.*, 1995). Likewise, although the general functional relationship between FALS and cell size is complex (Morel, 1991), within a specific group of cells, changes in FALS can provide information about changes in cell size (DuRand, 1995; see also the discussion of diel *Prochlorococcus* changes, below). Thus, we conclude that the observed changes in *Prochlorococcus* cellular red fluorescence and FALS during TS-II reflect a physiological response by these cells (specifically, an increase in chlorophyll content and cell size) to the changing conditions associated with the passage of the TIW. The proximal cause of this physiological response is not known at present (see "Ecological context" below). Note that we cannot exclude the possibility that the changes we observed were the result of shifts in *Prochlorococcus* species composition, analogous to the shifts that may occur with increasing depth (see above).

Bacterial cellular characteristics

As observed for photosynthetic groups, vertical profiles of cellular FALS among the heterotrophic bacteria were relatively invariant within and between the time-series [Fig. 6(C)]. Two days during TS-I [Julian days 83 and 97, both plotted separately in Fig. 6(C)] were obvious exceptions to this observation (see below).

The general increase in bacterial FALS at depth was superficially similar to the pattern observed among photosynthetic groups. However, in contrast to these latter groups, this increase was not the result of a simple increase of FALS in all cells, but rather reflected a change in the FALS frequency distribution among the bacterial cells (Fig. 8). Thus, for example, while the mode FALS of the bacterial population at depth on Julian day 281 was actually lower than at the surface, the presence of a greater proportion of large (high-FALS) cells at depth resulted in an increased mean FALS for that population [Fig. 8(A)]. In fact, although the total number of bacterial cells decreased with depth, the abundance of these larger cells actually increased [Fig. 8(B) and (C)]. The identity of these cells is not known at present.

In marked contrast to these results, Ducklow *et al.* (1995) reported that mean bacterial cell size (based on epifluorescence microscopy and image analysis) *decreased* with depth from 0 to 200 m. Because these cell size estimates were, of necessity, based on a relatively small number of cells, it is possible that they underestimate the contribution of the rare large cells that our data indicate may contribute significantly to total bacterial biomass, particularly at depth. Thus, the trend in mean size reported in that study may be related to the trend we observed in mode cellular FALS (which also decreased with depth). Alternatively, the large "bacterial" cells we observed could actually be small heterotrophic eukaryotes whose flow cytometric signatures were not clearly distinguishable from the general bacterial population. Further study is clearly necessary to identify and establish the importance of these cells.

With the exception of days 83 and 97 during TS-I, surface heterotrophic bacterial FALS changed little within and between cruises [Fig. 7(F)]. Again, this contrasts with the

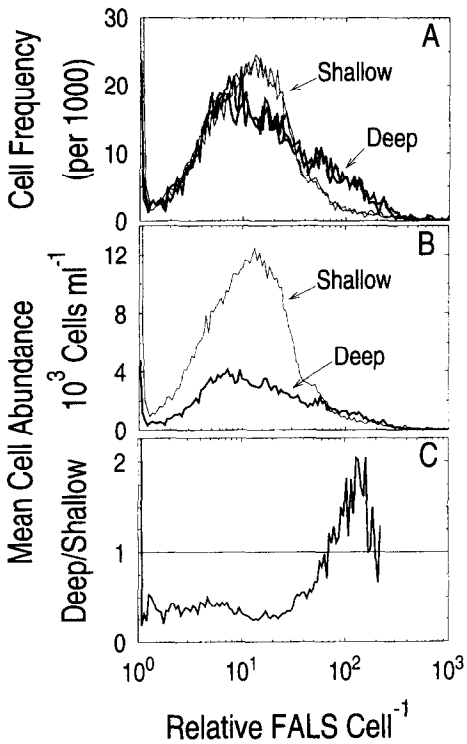

Fig. 8. Typical FALS frequency distributions for shallow and deep heterotrophic bacteria populations (from TS-II day 281, dawn profile). Panel (A) shows the relative frequency of bacteria cells with a given FALS for populations at depths of 0 and 15 m (narrow lines), and 175 and 200 m (heavy lines). (B) shows the mean concentration of cells ml^{-1} in each FALS class for these shallow and deep samples. (C) shows the ratio (deep/shallow) of cell concentrations in each FALS class. Note that the absolute concentration of larger (high-FALS) cells is greater at depth than at the surface.

observation of Ducklow *et al.* (1995) of larger mean cell size during TS-I than during TS-II at all depths. It is possible that mean bacterial cell size was the same at dawn (when we sampled) during both cruises, but increased over the course of the day at different rates, resulting in between-cruise differences at noon (when Ducklow *et al.* took their samples). Without further study, however, these two sets of observations cannot be unequivocally reconciled.

On days 83 and 97 during TS-I, mean bacterial FALS was dramatically higher than on other days [Fig. 7(F)], owing to the presence of a very abundant, apparently homogeneous, population of relatively large heterotrophic cells on these days (Fig. 9). Note that samples from each of these profiles were analyzed on different days. Furthermore, dusk samples from day 97 analyzed on yet another day also contained this population (data not shown). Finally, samples from other profiles analyzed on the same days as these did not appear to contain this population. Therefore, this phenomenon is unlikely to be the result of an analytical artifact. Based on their FALS signature, we estimate that the size of the cells in these populations was of the order of the size of *Prochlorococcus* or *Synechococcus* cells ($\sim$0.6–1 μm diameter). These populations were present at most depths on the days in question, and at times accounted for as much as 50% of the total heterotrophic bacterial cell

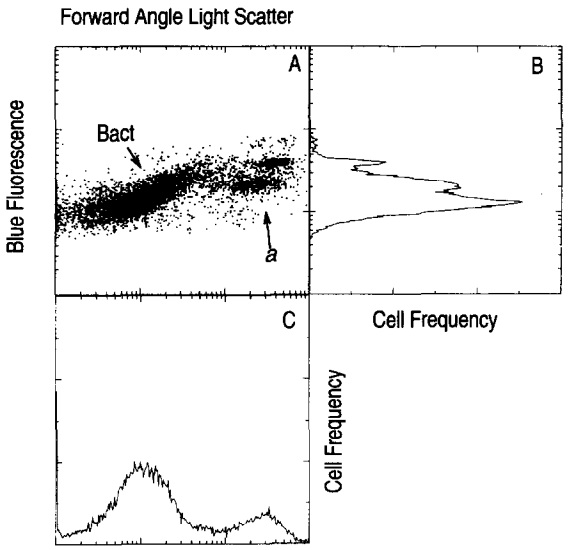

Fig. 9. Flow cytometric signature of the bacterial population at 90 m on day 83, showing the subpopulation of high-FALS cells (α). Red-fluorescing cells (including *Prochlorococcus*) and unstained particles have been excluded. (A) Dot plot of blue fluorescence (DNA) vs FALS (each dot represents a single cell with the corresponding combination of parameter values); (B) DNA frequency distribution of the entire population; and (C) FALS frequency distribution of the entire population. The high-FALS subpopulation is evident as a second peak in the FALS distribution, and as two distinct peaks in the DNA distribution, possibly corresponding to "g1 " and "g2" cells.

count; their appearance was not obviously correlated with any environmental change. The relationship between these dense populations and the relatively rare large cells that appear at depth in most of our depth profiles is unknown at present. In any case, these data point to the occurrence of abrupt and potentially significant shifts in the structure of the microbial community during TS-I, in the absence of any other obvious biotic or abiotic changes.

Biomass estimates

The contribution of heterotrophic bacteria, *Prochlorococcus*, *Synechococcus* and ultraphytoplankton to total community biomass can be roughly estimated by using literature values for the mean carbon content per cell for each of these groups (Table 2). For this purpose, we have adopted the C cell^{-1} values used by Campbell *et al.* (1994). The resultant estimates of photosynthetic pico- plus ultraplankton standing stock (Table 2) correspond, respectively, to 91 and 88% of the average total phytoplankton standing stock during TS-I and TS-II, as estimated by Murray *et al.* (1994) based on bulk chlorophyll measurements (assuming C:chlorophyll $a = 58$).

On a depth-integrated basis, ultraphytoplankton accounted for the largest fraction of the photosynthetic carbon standing stock (52 and 65% during TS-I and TS-II, respectively). *Prochlorococcus* populations contributed 41 and 27%, respectively, and *Synechococcus* contributed between 7 and 8%. This contribution by ultraphytoplankton is considerably larger than that estimated for the subtropical North Pacific (where it was ~27%, Campbell *et al.*, 1994), but comparable to the estimate made by Li *et al.* (1992) for the Sargasso Sea.

Table 2. Estimated depth-integrated standing stocks of pico- and ultraplankton groups and bacteria during TS-I and TS-II

	Prochlorococcus	*Synechococcus*	Ultraphytoplankton	Photosynthetic pico + ultra*	Heterotrophic bacteria
Assumed biomass per cell (fg C)†					
	53	250	2100		20
Standing stock (mmol C m^{-2})‡					
TS-I	53	9	66	128	101
TS-II	40	11	95	145	107
Proportion of total photosynthetic pico + ultra* (%)					
TS-I	41	7	52		79
TS-II	27	8	65		74

*Photosynthetic pico + ultra = *Prochlorococcus* + *Synechococcus* + ultraphytoplankton.
†From Campbell *et al.* (1994).
‡Based on integrated cell abundances from Table 1.

Calculated bacterial standing stocks were 2–3 times higher than *Prochlorococcus* standing stocks, but were slightly less than calculated total photosynthetic pico- plus ultraplankton standing stocks. This agrees generally with previous estimates of the relative magnitude of photosynthetic and bacterial standing stocks in non-oligotrophic environments (see Cho and Azam, 1990), and with more recent estimates (which include *Prochlorococcus*) in oligotrophic areas (Li *et al.*, 1992; Campbell *et al.*, 1994).

Summed chlorophyll fluorescence

In order to estimate the contribution of each photosynthetic group to total pico- plus ultraplankton chlorophyll biomass, we can consider their "summed red fluorescence", calculated in each sample as the product of mean red fluorescence per cell and cell concentration. Because this analysis involves comparing red fluorescence across different taxonomic groups, conclusions must be drawn with caution (Sosik *et al.*, 1989; Perry and Porter, 1989). Nevertheless, flow cytometric summed red fluorescence has been shown to be reasonably correlated with measured bulk chlorophyll in the field (Li *et al.*, 1993; Zettler *et al.*, 1996), and, therefore, can be useful for making order-of-magnitude estimates of the relative contribution of different groups to total chlorophyll standing stock. In fact, the total summed red fluorescence values in this study are well correlated with bulk chlorophyll *a* measurements of the same water ($r = 0.81$, $p < 0.01$) (Bidigare and Ondrusek, 1996).

Prochlorococcus summed red fluorescence (integrated over the top 120 m) was significantly higher during TS-I than during TS-II (Fig. 10 and Table 3). This difference reflected not only the generally higher depth-integrated *Prochlorococcus* cell numbers during the first cruise, but also the fact that a larger proportion of those cells were found at greater depths, where fluorescence per cell is higher. Despite the generally lower depth-integrated ultraphytoplankton cell numbers during TS-I, ultraphytoplankton depth-integrated red fluorescence was comparable on both cruises. Again, this is the result of a greater proportion of cells at depth during TS-I relative to TS-II. Finally, *Synechococcus* summed red fluorescence was lower on average during TS-I than it was during TS-II (Table 3). In this case, changes in depth-integrated fluorescence paralleled changes in cell number.

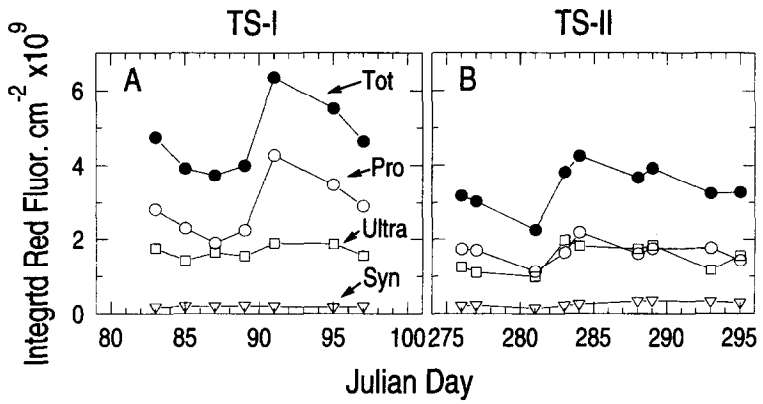

Fig. 10. Depth-integrated red fluorescence for *Prochlorococcus* (○), *Synechococcus* (▽), ultraphytoplankton (□) and total pico- plus ultraplankton (●) (= sum of the three groups above) over the course of TS-I (A) and TS-II (B). Each point represents the single value calculated for a given dawn cast (integrated to 120 m), based on flow cytometrically measured per cell fluorescence and cell concentration and expressed in relative fluorescence units $cm^{-2} \times 10^9$.

On average, *Prochlorococcus* fluorescence accounted for 60 and 49% of the total depth-integrated pico- plus ultraplankton fluorescence during TS-I and TS-II, respectively (Fig. 10 and Table 3). The mean ultraphytoplankton contributions were 36 and 44% during these same periods. *Synechococcus* were never responsible for more than 10% of the overall picoplankton red fluorescence (average contribution was 4.3 and 7.6% during TS-I and TS-II, respectively). Insofar as these calculations indicate that both *Prochlorococcus* and eukaryotic ultraphytoplankton contribute significantly to total photosynthetic biomass, they are consistent with the estimates of group-specific carbon biomass calculated above. Quantitative differences between these estimates in terms of the proportion of biomass contributed by these two groups may reflect errors in the assumed carbon cell quota and/or differences in the carbon:chlorophyll ratio or chlorophyll-specific absorbance cross-sections among groups and between different depths.

Depth-integrated total pico- plus ultraplankton red fluorescence was 28% lower during TS-II than during TS-I, suggesting that the overall chlorophyll biomass of these groups was somewhat greater during TS-I (subject to the same caveats listed above) (Fig. 10 and Table

Table 3. Comparison of daily water column-integrated (120 m) summed red fluorescence and variability between TS-I and TS-II (mean ± SD, × 10^8 relative fluorescence units cm^{-2}*)*

	n	*Prochlorococcus*	*Synechococcus*	Ultraphytoplankton	Total
TS-I	7	28.4±8.16	1.92±0.16	16.7±1.79	47.0±9.54
TS-II	9	16.6±2.84	2.58±0.69	14.9±3.71	34.0±5.91
Change (TS-I→TS-II)*		−42%	+34%	(−11%)	−28%
Means†		$p<0.002$	$p<0.05$	NS	$p<0.01$
Variances‡		$p<0.01$	$p<0.002$	$p<0.05$	NS

*Change in time-series average, values in parentheses not significant.
†Mann–Whitney U-test comparing time-series means.
‡Two-tailed *F*-test comparing time-series variances.

3). This difference was largely the result of changes in summed *Prochlorococcus* fluorescence between these cruises, and contrasts the conclusion of Bidigare and Ondrusek (1996) that picoplankton chlorophyll biomass was unchanged between the two time-series.

Dawn–dusk comparisons: Prochlorococcus *growth rates*

By comparing the DNA frequency distributions of *Prochlorococcus* populations at dawn and dusk, lower bound estimates of the growth rates of these populations can be calculated. We made such comparisons on 4 days during TS-I and 3 days during TS-II (e.g. Fig. 11). At dawn, *Prochlorococcus* populations are comprised almost exclusively of "g1" cells, having one complement of DNA and, therefore, not ready to divide. At dusk many "s" and "g2" cells, with higher DNA contents, are present [Fig. 11(B)] (see also Vaulot *et al.*, 1995). Note that we use the terms "g1", "s" and "g2" as a simplified way of identifying subpopulations of cells according to their DNA content, and not to refer to cell cycle stages *per se* (Binder and Chisholm, 1995). Because there are essentially no s or g2 cells left at dawn, any such cells observed at dusk must have divided to form new g1 cells during the night. Therefore, we can use the proportion of s + g2 cells present at dusk to estimate the minimum intrinsic growth rate (μ_{min}) that the population could have achieved during the day in question (see Materials and Methods). The growth rate so calculated is a minimum estimate of the true growth rate because it assumes that all of the cells that are going to divide on a

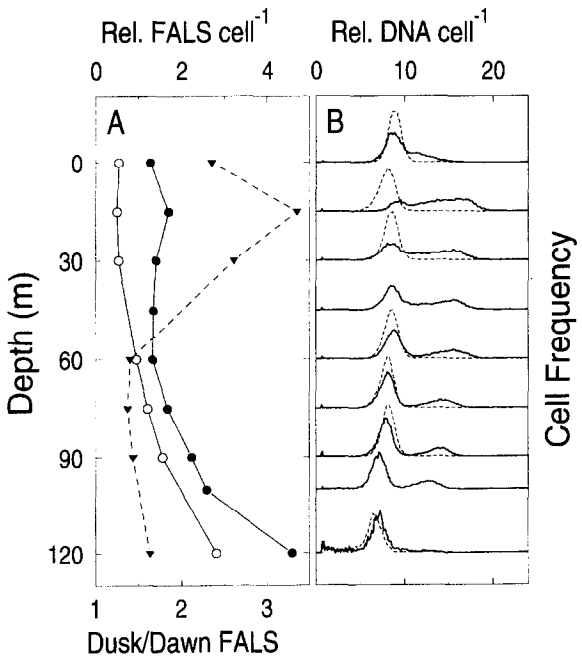

Fig. 11. Typical vertical distribution of *Prochlorococcus* per cell FALS (A) and DNA distributions (B). Data for dawn [○ in (A), broken line in (B)] and dusk [● in (A), solid line in (B)] casts on Julian day 83 during TS-I. The broken line in (A) shows the ratio of dusk:dawn FALS. DNA distributions are derived from linearized histograms of *Prochlorococcus* Hoechst-33342 fluorescence (see Materials and Methods).

given day are counted at dusk (i.e. that no cell division occurs between dawn and dusk, and no cells begin DNA replication in preparation for division after dusk) (McDuff and Chisholm, 1982; Antia *et al.*, 1990; Vaulot, 1992). Because any violation of these assumptions will lower the calculated growth rate, μ_{min} represents a robust lower-bound estimate of actual *Prochlorococcus in situ* growth rates. Note that this estimate refers to the intrinsic specific growth rate of the population, independent of grazing and other loss terms.

The calculated *Prochlorococcus* μ_{min} values in this study ranged from 0.28 to 0.52 day^{-1} at the surface, generally were maximal at 15 or 30 m, where they ranged from 0.49 to 0.64 day^{-1} and decreased with depth thereafter (Fig. 12). There was no indication of significant differences in *Prochlorococcus* growth rates between TS-I and TS-II, or over the course of TS-II. The highest minimum specific growth rates calculated here approach 0.69 day^{-1}, or one doubling per day. These rates are near the maximum specific growth rates achievable in nutrient replete *Prochlorococcus* laboratory cultures (Moore *et al.*, 1995), and imply that the field populations, at least those at 15–30 m depth, are not nutrient-limited.

Vaulot *et al.* (1995) used DNA distributions from samples taken at 3-h intervals on selected days during TS-I and TS-II to more accurately estimate *Prochlorococcus* growth rates. Those estimates are comparable to the rates reported here, and vary with depth in a similar way. The data of Vaulot *et al.* (1995) as well as Dusenberry (1995) confirm that division in natural *Prochlorococcus* populations is tightly phased and is restricted to the late afternoon and early evening. However, Vaulot *et al.* (1995) also show that the daily peak in the fraction of s + g2 *Prochlorococcus* cells occurs prior to dusk below depths of 30–45 m. This means that some cell division probably occurred prior to our dusk sampling and, therefore, that our calculated μ_{min} values at these depths are underestimates of the true growth rate (possibly by as much as 50%).

Estimates of *Prochlorococcus* growth rates during the time-series cruises also were made by DuRand (1995), based on diel changes in average *Prochlorococcus* FALS. The magnitude and depth-distribution of these estimates agree well with those presented here.

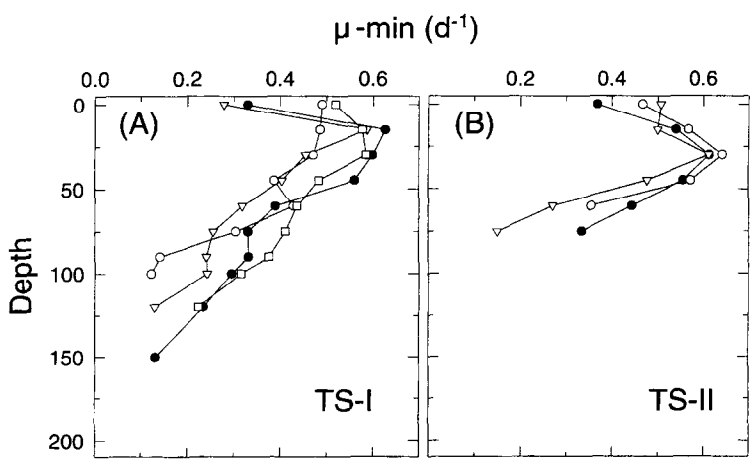

Fig. 12. Vertical profiles of estimated minimum specific growth rates among *Prochlorococcus* during TS-I (A) and TS-II (B). Rates based on the proportion of "g2" + "s" cells at dusk (see text). In (A), data are for Julian days 83 (▽), 87 (●), 91 (□) and 97 (○); in (B) they are for days 276 (●), 281 (○) and 293 (▽).

Finally, Landry *et al.* (1995a) used dilution experiments to estimate *Prochlorococcus* growth rates at the equator in late August. The single value from 40 m depth (0.62 day^{-1}) is comparable to the *in situ* estimates reviewed above, whereas two 10 m values (−0.05 and 0.26 day^{-1}, based on "relative grazing" analysis) are somewhat low relative to these estimates.

In the present study, FALS per *Prochlorococcus* cell was greater at dusk than at dawn for all depths, on all days [Fig. 11(A)]. This is taken to reflect cell growth during the day (which would increase FALS per cell), followed by cell division at night (which would decrease FALS per cell) among the *Prochlorococcus*. Similar patterns have been observed in *Synechococcus* and ultra- and nanoplankton, as well as in *Prochlorococcus* (Olson *et al.*, 1990b; Dusenberry, 1995; DuRand, 1995; DuRand and Olson, 1996).

The magnitude of the increase in FALS per cell from dawn to dusk (expressed as a ratio) was well correlated with the μ_{min} calculated for the same pair of samples ($r = 0.86$, $p < 0.01$) (Fig. 13). Note that these two measures are analytically independent of each other. This correlation reflects a relationship between the magnitude of increase in biomass during the day and the extent of cell division the following night, as might be expected. These observations support the notion that changes in *Prochlorococcus* forward light scatter can be used to estimate *in situ* growth rates in the absence of DNA data (see DuRand, 1995).

Conversely, the observed correlation between light scatter change and μ_{min} can be used to relate FALS to *Prochlorococcus* cell volume, at least to a first approximation. From a Model II regression of the data in Fig. 13, we estimate that the FALS ratio for a *Prochlorococcus* population growing at 0.69 day^{-1} (i.e. one doubling per day) = 3.55. Given that the mean cell volume of a well-phased population growing at this rate must double between bursts of division, and assuming that: (1) no cell growth (or shrinkage) occurs between dusk and dawn, and (2) that FALS $\propto$ (cell volume)$^{\beta}$ [where β is a constant specific for the cell type in question and the optical configuration employed here (Morel, 1991)], this leads to the calculation of β as 1.83. This estimated value of β is consistent with theoretical expectations

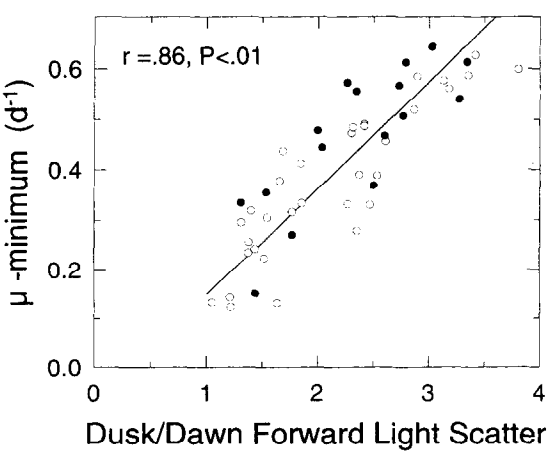

Fig. 13. The relationship between calculated minimum *Prochlorococcus*-specific growth rate and the ratio of dusk to dawn per cell FALS during TS-I (○) and TS-II (●). Each point represents a single depth from a single dawn–dusk pair of profiles; the correlation statistics and Model II regression line are for all data combined.

for particles of the order of 0.6 μm in diameter (Morel, 1991), and is remarkably close to the value of 1.80 determined empirically for *Synechococcus* by DuRand (1995).

As shown above, *Prochlorococcus* FALS per cell increased by a factor of 4.5 from 0 to 120 m depth during both time-series [Fig. 6(A)]. Using the derived value of β, this corresponds to a change in cell volume by a factor of approximately 2.3. At the same time, the red fluorescence per cell in these populations increased by an average factor of 16–23 [Fig. 5(A)]. Thus, assuming that within the *Prochlorococcus* populations in these samples, red fluorescence is proportional to chlorophyll *a* content and carbon content is proportional to biovolume, the expected carbon:chlorophyll ratio changes by a factor of 7–10 between the surface and the 0.1% light level. Although the relationships between FALS and cell volume, and between red fluorescence and pigment content, clearly require further investigation, these calculations imply that estimates of *Prochlorococcus* standing stock based on pigment concentrations or cell numbers alone, including those in this paper, should be viewed with caution.

Similar calculations can be applied to the changes observed in *Prochlorococcus* FALS and red fluorescence in response to the TIW during TS-II [Fig. 7(A) and (D)]. In this case, both parameters increased by factor of approximately 1.7. This corresponds to an increase in cell volume of 1.3 and, therefore (given the same assumptions as above), a change in the carbon:chlorophyll ratio of approximately 1.3.

Ecological context

To what extent are the pico- and ultraplankton data we have presented here related to the community-level changes observed during the JGOFS EqPac study? In terms of low-frequency changes (expressed as differences between the two time-series), our observations of decreased *Prochlorococcus* standing stock and increased or unchanged ultraphytoplankton standing stock between TS-1 and TS-II are consistent with the suggestion that there was a shift toward larger phytoplankton groups during TS-II (Murray *et al.*, 1994; Bidigare and Ondrusek, 1996; Landry *et al.*, 1996).

The change in *Prochlorococcus* standing stock between TS-I and TS-II was largely a reflection of a shoaling of the vertical distribution of these cells during TS-II. Yet the cellular characteristics of these populations were similar at similar depths. It therefore appears unlikely that differences in the mixing regime, which should be manifested in differences in cellular red fluorescence (Dusenberry, 1995), are responsible for this shoaling. It may be that the increased rate of upwelling during TS-II in effect diluted the deeper, more slowly growing, populations to extinction. Ultraphytoplankton distributions, which were also shallower during TS-II, could have been likewise affected, while *Synechococcus* populations, which showed no difference, may already have been restricted to shallower depths by light limitation.

Chlorophyll-specific primary production (calculated from 24-h ^{14}C incubations) was higher during TS-II relative to TS-I, suggesting that the average primary producer growth rate was higher during TS-II (Barber *et al.*, 1994; Murray *et al.*, 1994). Phytoplankton growth rates estimated from dilution experiments support this suggestion (Landry *et al.*, 1995b; Verity *et al.*, 1996). Our limited data for *Prochlorococcus* growth rates do not reflect this trend: no obvious difference was observed between the two time-series. Again, this is consistent with the idea that the observed changes in community primary production resulted from a stimulation of larger size classes, rather than a change in the activity of the

community as a whole (Murray *et al.*, 1994). Note, however, that subtle changes in *Prochlorococcus* growth rates could have been obscured from our analysis by concomitant shifts in the timing of cell division.

With regard to high-frequency (within-cruise) variability, Murray *et al.* (1994) showed that a systematic change in total chlorophyll *a* and primary production occurred during TS-II, coinciding with the passage of a TIW. Although there is a suggestion in our study of concomitant increases in integrated cell numbers and/or bulk red fluorescence for all three photosynthetic groups during the same period, changes of similar magnitude and consistency occurred during TS-I. Thus, while there is a 2-fold increase in integrated pico- plus ultraplankton red fluorescence between days 281 and 284 (corresponding approximately to the time when increases in P_{max} and chlorophyll *a* at the depth of P_{max} were observed; Murray *et al.*, 1994) [Fig. 10(B)], there is a similarly dramatic increase in total summed red fluorescence between days 89 and 91 during TS-I [Fig. 10(A)]. Therefore, it seems inappropriate to draw any connection between the passage of the TIW and the observed changes in pico- and ultraplankton abundance or summed red fluorescence.

In contrast, the clear change in both chlorophyll content per cell and cell size (inferred from red fluorescence and FALS) among *Prochlorococcus* cells during TS-II was probably the result of physiological changes associated with the passage of the TIW. No such changes in these parameters were observed over the course of TS-I. It is not yet known what factors were directly responsible for the changes in community-level characteristics that were correlated with the passage of this wave (Murray *et al.*, 1994); likewise, the proximal cause of the physiological changes among *Prochlorococcus* cells is not known. One possibility is that as the upwelling core traversed the study site, water rich in iron (from the Equatorial Undercurrent) was injected into the surface (see Gordon *et al.*, 1996). Increases in Fe have been shown to result in increased cell size and fluorescence among pico- and ultraplankton groups in bottle enrichment experiments in this area (Zettler *et al.*, 1996). Our observation of similar *in situ* changes are consistent with the suggestion that picoplankton cells are iron-stressed in the surface waters of the equatorial Pacific (Martin *et al.*, 1994; Kolber *et al.*, 1994).

Evidence for physiological changes notwithstanding, our analysis (as well as that of Vaulot *et al.*, 1995) suggests that *Prochlorococcus* intrinsic growth rates did not change in response to the passage of the instability wave. Again, these results are echoed by iron-enrichment bottle experiments, in which no change in net growth rates could be discerned among the pico- and ultraphytoplankton despite increases in red fluorescence and/or FALS (Zettler *et al.*, 1996). Thus, the presence of a physiological change in an *in situ* phytoplankton population may not necessarily imply a change in the specific growth rate of that population.

The relatively constant chlorophyll-specific primary production over the course of TS-II has been taken as evidence that the observed changes in the absolute rate of production (i.e. mg C m^{-2} day^{-1}) associated with the passage of the TIW were not driven by physiological changes among the phytoplankton (Murray *et al.*, 1994). This conclusion should be viewed with caution, however. In the case of *Prochlorococcus*, the physiological changes that we hypothesize to have occurred involved increases in both carbon and chlorophyll content (as deduced from increases in FALS and red fluorescence per cell, respectively), and would, therefore, have been difficult to discern in terms of the ratio of these parameters (or, presumably, in terms of chlorophyll-specific production). Although our data suggest that these physiological changes were not, in fact, reflected in increased specific growth rates, the

inferred increase in biomass per cell (in conjunction with constant cell abundance) would nevertheless have resulted in increased total *Prochlorococcus* biomass and production.

Acknowledgements—We thank the captain and crew of R.V. *Thompson*, and the chief scientists of the time-series cruises, Michael Roman and Michael Bacon, for their co-operation and support. We gratefully acknowledge the contribution of Erik Zettler to our research effort during both cruises. Carole Duval contributed to the modification of the flow cytometer and development of our analytical protocols. Lana Aref and Elizabeth Mann assisted with data analysis.

This work was supported in part by NSF grants OCE-9022285, OCE-9223793, OCE-9000043, OCE-9302529 and DIR-9101361 (to S. W. Chisholm), and OCE-9024380 (to R. J. Olson). This is U.S. JGOFS contribution no. 208 and Woods Hole Oceanographic Institution contribution no. 9103.

REFERENCES

Antia A. N., E. J. Carpenter and J. Chang (1990) Species-specific phytoplankton growth rates via diel DNA synthesis cycles. III. Accuracy of growth rate measurement in the dinoflagellate *Prorocentrum minimum*. *Marine Ecology Progress Series*, **63**, 273–279.

Barber R. T., J. W. Murray and J. J. McCarthy (1994) Biogeochemical interactions in the equatorial Pacific. *Ambio*, **23**, 62–66.

Bidigare R. R. and M. E. Ondrusek (1996) Spatial and temporal variability of phytoplankton pigment distributions in the central equatorial Pacific ocean. *Deep-Sea Research II*, **43**, 809–833.

Binder B. J. and S. W. Chisholm (1995) Cell cycle regulation in marine *Synechococcus* sp. strains. *Applied and Environmental Microbiology*, **61**, 708–717.

Blanchot J., M. Rodier and A. Le Bouteiller (1992) Effect of El Niño Southern Oscillation events on the distribution and abundance of phytoplankton in the western Pacific tropical ocean along 165°E. *Journal of Plankton Research*, **14**, 137–156.

Campbell L. and D. Vaulot (1993) Photosynthetic picoplankton community structure in the subtropical North Pacific Ocean near Hawaii (station ALOHA). *Deep-Sea Research*, **40**, 2043–2060.

Campbell L., H. A. Nolla and D. Vaulot (1994) The importance of *Prochlorococcus* to community structure in the central North Pacific Ocean. *Limnology and Oceanography*, **39**, 954–961.

Chavez F. P. (1989) Size distribution of phytoplankton in the central and eastern tropical Pacific. *Global Biogeochemical Cycles*, **3**, 27–35.

Chavez F. P., K. R. Buck, K. H. Coale, J. H. Martin, G. R. DiTullio, N. A. Welschmeyer, A. C. Jacobson and R. T. Barber (1991) Growth rates, grazing, sinking, and iron limitation of equatorial Pacific phytoplankton. *Limnology and Oceanography*, **36**, 1816–1833.

Chisholm S. W. (1992) Phytoplankton size. In: *Primary production and biogeochemical cycles in the sea*, P. G. Falkowski and A. D. Woodhead, editors. Plenum Press, New York, pp. 213–237.

Cho B. C. and F. Azam (1990) Biogeochemical significance of bacterial biomass in the ocean's euphotic zone. *Marine Ecology Progress Series*, **63**, 253–259.

DuRand M. (1995) Phytoplankton growth and diel variations in beam attenuation through individual cell analysis. Ph.D. thesis, Massachusetts Institute of Technology–Woods Hole Oceanographic Institution Joint Program in Oceanography, 263 pp.

DuRand M. D. and R. J. Olson (1996) Contributions of phytoplankton light scattering and cell concentration changes to diel variations in beam attenuation in the equatorial Pacific from flow cytometric measurements of pico-, ultra- and nanoplankton. *Deep-Sea Research II*, **43**, 891–906.

Ducklow H. W., H. L. Quinby and C. A. Carlson (1995) Bacterioplankton dynamics in the equatorial Pacific during the 1992 El Niño. *Deep-Sea Research II*, **42**, 621–638.

Dusenberry J. (1995) Picoplankton photoacclimation and mixing in the surface oceans. Ph.D. thesis, Massachusetts Institute of Technology–Woods Hole Oceanographic Institution Joint Program in Oceanography, 301 pp.

Feely R. A., R. H. Gammon, B. A. Taft, P. E. Pullen, L. S. Waterman, T. J. Conway, J. F. Gendron and D. P. Wisegarver (1987) Distribution of chemical tracers in the eastern equatorial Pacific during and after the 1982–1983 El Niño/Southern Oscillation event. *Journal of Geophysical Research*, **92**, 6545–6558.

Gordon R. M., K. H. Coale and K. W. Johnson (1996) Iron distribution in the equatorial Pacific: implications for new production. *Limnology and Oceanography*, in press.

Kolber Z. S., R. T. Barber, K. H. Coale, S. E. Fitzwater, R. M. Greene, K. S. Johnson, S. Lindley and P. G. Falkowski (1994) Iron limitation of phytoplankton photosynthesis in the equatorial Pacific Ocean. *Nature*, **371**, 145–149.

Landry M. R., J. Kirshtein and J. Constantinou (1995) A refined dilution technique for measuring the community grazing impact of microzooplankton, with experimental tests in the central equatorial Pacific. *Marine Ecology Progress Series*, **120**, 53–63.

Landry M. R., J. Constantinou and J. Kirshtein (1995) Microzooplankton grazing in the central equatorial Pacific during February and August 1992. *Deep-Sea Research II*, **42**, 657–671.

Landry M. R., J. Kirshtein and J. Constantinou (1996) Abundances and distributions of picoplankton populations in the central equatorial Pacific from 12°N to 12°S, 140°W. *Deep-Sea Research II*, **43**, 871–890.

Li W. K. W. and A. M. Wood (1988) Vertical distribution of North Atlantic ultraphytoplankton: analysis by flow cytometry and epifluorescence microscopy. *Deep-Sea Research*, **35**, 1615–1638.

Li W. K. W., P. M. Dickie, B. D. Irwin and A. M. Wood (1992) Biomass of bacteria, cyanobacteria, prochlorophytes and photosynthetic eukaryotes in the Sargasso Sea. *Deep-Sea Research*, **39**, 501–519.

Li W. K. W., T. Zoliary, Y. Z. Yacobi and A. M. Wood (1993) Ultraphytoplankton in the eastern Mediterranean Sea: towards deriving phytoplankton biomass from flow cytometric measurements of abundance, fluorescence and light scatter. *Marine Ecology Progress Series*, **102**, 79–87.

Longhurst A. R. (1991) Role of the marine biosphere in the global carbon cycle. *Limnology and Oceanography*, **36**, 1507–1526.

Martin J. H. *et al.* (1994) Testing the iron hypothesis in ecosystems of the equatorial Pacific Ocean. *Nature*, **371**, 123–129.

McDuff R. E. and S. W. Chisholm (1982) The calculation of *in situ* growth rates of phytoplankton populations from fractions of cells undergoing mitosis: a clarification. *Limnology and Oceanography*, **27**, 783–788.

Monfort P. and B. Baleux (1992) Comparison of flow cytometry and epifluorescence microscopy for counting bacteria in aquatic ecosystems. *Cytometry*, **13**, 188–192.

Monger B. C. and M. R. Landry (1993) Flow cytometric analysis of marine bacteria with Hoechst 33342. *Applied and Environmental Microbiology*, **59**, 905–911.

Moore L. R., R. Goericke and S. W. Chisholm (1995) Comparative physiology of *Synechococcus* and *Prochlorococcus*: influence of light and temperature on growth, pigments, fluorescence and absorptive properties. *Marine Ecology Progress Series*, **116**, 259–275.

Morel A. (1991) Optics of marine particles and marine optics. In: *Particle analysis in oceanography. NATO ASI Series G, ecological sciences*, Vol. 27, S. Demers, editor. Springer, New York, pp. 141–188.

Murray J. W., M. W. Leinen, R. A. Feely, J. R. Toggweiler and R. Wanninkhof (1993) EqPac: a process study in the central equatorial Pacific. *Oceanography*, **5**, 134–142.

Murray J. W., R. T. Barber, M. R. Roman, M. P. Bacon and R. A. Feely (1994) Physical and biological controls on carbon cycling in the equatorial Pacific. *Science*, **266**, 58–65.

Olson R., S. W. Chisholm, E. R. Zettler, M. A. Altabet and J. A. Dusenberry (1990) Spatial and temporal distributions of prochlorophyte picoplankton in the North Atlantic Ocean. *Deep-Sea Research*, **37**, 1033–1051.

Olson R. J., S. W. Chisholin, E. R. Zettler and E. V. Armbrust (1990) Pigments, size, and distribution of *Synechococcus* in the North Atlantic and Pacific Oceans. *Limnology and Oceanography*, **35**, 45–58.

Olson R. L., E. R. Zettler and M. D. DuRand (1993) Phytoplankton analysis using flow cytometry. In: *Handbook of methods in aquatic microbial ecology*, P. F. Kemp, B. F. Sherr, E. B. Sherr and J. J. Cole, editors. Lewis Publishers, Boca Raton, FL, pp. 175–186.

Peña M. A., M. R. Lewis and W. G. Harrison (1990) Primary productivity and size structure of phytoplankton biomass on a transect of the equator at 135°W in the Pacific Ocean. *Deep-Sea Research*, **37**, 295–315.

Perry M. J. and S. M. Porter (1989) Determination of the cross-section absorption coefficient of individual phytoplankton cells by analytical flow cytometry. *Limnology and Oceanography*, **34**, 1727–1738.

Robertson B. R. and D. K. Button (1989) Characterizing aquatic bacteria according to population, cell size and apparent DNA content by flow cytometry. *Cytometry*, **10**, 7076.

Shapiro L. P. and R. R. L. Guillard (1986) Physiology and ecology of the marine eukaryotic ultraplankton. *Canadian Bulletin of Fisheries and Aquatic Sciences*, **214**, 371–389.

Shimada A., T. Hasegawa, I. Umeda, N. Kadoya and T. Maruyania (1993) Spatial mesoscale patterns of West Pacific picophytoplankton as analyzed by flow cytometry: their contribution to subsurface chlorophyll maxima. *Marine Biology*, **115**, 209–215.

Sosik H. M., S. W. Chisholm and R. J. Olson (1989) Chlorophyll fluorescence from single cells: Interpretation of flow cytometric signals. *Limnology and Oceanography*, **34**, 1749–1761.

Stockner J. G. and N. J. Antia (1986) Algal picoplankton from marine and freshwater ecosystems: A multidisciplinary perspective. *Canadian Journal of Fisheries and Aquatic Sciences*, **43**, 2472–2503.

Suzuki M. T., E. B. Sherr and B. F. Sherr (1993) DAPI direct counting underestimates bacterial abundances and average cell-size compared to AO direct counting. *Limnology and Oceanography*, **38**, 1566–1570.

Vaulot D. (1992) Estimate of phytoplankton division rates by the "mitotic index" method: the f_{max} approach revisited. *Limnology and Oceanography*, **37**, 644–649.

Vaulot D., C. Courties and F. Partensky (1989) A simple method to preserve oceanic phytoplankton for flow cytometric analyses. *Cytometry*, **10**, 629–635.

Vaulot D., F. Partensky, J. Neveux, R. F. C. Mantoura and C. A. Llewellyn (1990) Winter presence of prochlorophytes in surface waters of the northwestern Mediterranean Sea. *Limnology and Oceanography*, **35**, 1156–1164.

Vaulot D., D. Marie, R. J. Olson and S. W. Chisholm (1995) Growth of *Prochlorococcus*, a photosynthetic prokaryote, in the equatorial Pacific ocean. *Science*, **268**, 1480–1482.

Veldhuis M. J. W. and G. W. Kraay (1990) Vertical distribution and pigment composition of a picoplanktonic prochlorophyte in the subtropical North Atlantic: a combined study of HPLC-analysis of pigments and flow cytometry. *Marine Ecology Progress Series*, **68**, 121–127.

Verity P. G., D. K. Stoecker, M. E. Sieracki and J. R. Nelson (1996) Microzooplankton grazing of primary production at 140°W in the equatorial Pacific. *Deep-Sea Research II*, **43**, 1227–1255.

Weisse T. (1993) Dynamics of autotrophic picoplankton in marine and freshwater ecosystems. In: *Advances in microbial ecology*, Vol. 13, J. G. Jones, editor. Plenum Press, New York, pp. 327–370.

Zettler E. R., R. J. Olson, B. J. Binder, S. W. Chisholm, S. E. Fitzwater and R. M. Gordon (1996) Iron-enrichment bottle experiments in the equatorial Pacific: responses of individual phytoplankton cells. *Deep-Sea Research II*, **43**, 1017–1029.